Available online at www.sciencedirect.com
SCIENCE DIRECT®
Journal of Crystal Growth 265 (2004) 1–7
JOURNAL OF CRYSTAL GROWTH
www.elsevier.com/locate/jcrysgro

Effects of growth pause on the structural and optical properties of InGaAsN–InGaAsP quantum well

Jeng-Ya Yeh[a,*], Nelson Tansu[b], Luke J. Mawst[a]

[a] *Department of Electrical and Computer Engineering, Reed Center for Photonics, University of Wisconsin-Madison, 1415 Engineering Drive, Madison, WI 53706, USA*

[b] *Department of Electrical and Computer Engineering, Center for Optical Technologies, Lehigh University, 7 Asa Drive, Bethlehem, PA 18015, USA*

Received 7 August 2003; accepted 9 January 2004
Communicated by C.R. Abernathy

Abstract

Optical and structural characterizations were conducted on an InGaAsN quantum well (QW) with large energy bandgap barrier material consisting of InGaAsP ($E_g = 1.62$ eV) grown by metalorganic chemical vapor deposition. A growth pause annealing technique substantially improves both the structural and the optical quality of the QW. With an optimum growth pause of 14 s, surface roughness reduces by 50% and photoluminescence intensity increases 25 times compared with the sample undergoing a 3-s growth pause. No significant emission wavelength blue shift was observed, indicating this growth pause annealing process involves a mechanism different from that of the conventional post-growth thermal annealing of InGaAsN QW. Preliminary results on InGaAsN-active diode lasers employing InGaAsP barrier material indicate performance is limited by nonradiative recombination.

PACS: 81.40.E; 68.35.C; 81.15.G; 45.55.P

Keywords: A1. Annealing; A1. Growth interruption; A1. Surface morphology; A3. MOCVD; B2. InGaAsN; B3. Semiconductor lasers

1. Introduction

First proposed by Kondow et al. in 1997 [1], InGaAsN material systems have generated increasing interest for achieving high-performance quantum well (QW) lasers with emission wavelengths around 1300 nm for the application of telecommunication transmitters [2–4]. Since then, room-temperature threshold current density of 1300-nm InGaAsN QW lasers has been successfully reduced to approximately 210–270 A/cm^2 [2–4]. One of the methods to improve InGaAsN material quality is through post-growth rapid thermal annealing which has been widely used to enhance the InGaAsN QW optical characteristics. Several experimental results have been previously conducted to determine the effects of various device structures, material compositions and annealing conditions on both optical and structural properties of InGaAsN [5–8].

*Corresponding author. Tel.: +608-265-5403; fax: +608-265-4623.
E-mail address: jyeh@cae.wisc.edu (J.-Y. Yeh).

0022-0248/$ - see front matter © 2004 Elsevier B.V. All rights reserved.
doi:10.1016/j.jcrysgro.2004.01.022

In this work, we report a new annealing process performed during the growth pause introduced before and after the QW [9,10] which was found to be critical for structures containing InGaAsN QW and InGaAsP barriers. A systematic optical luminescence and surface morphology characterization study was conducted to understand the underlying mechanism. The intention of utilizing high-energy bandgap InGaAsP of 1.62 eV as the barriers surrounding the QW is to improve the carrier confinement in the QW. Studies have shown that the valence band offset of InGaAsN–GaAs is much smaller than InGaAs–GaAs [11] and a possible hole leakage process may contribute to the increased temperature sensitivity of the threshold current density and the external differential quantum efficiency found in high-performance InGaAsN QW lasers [12]. Previously, we have shown that by utilizing the InGaAsN QW structures with GaAsP ($E_g = 1.55$ eV) barriers, low threshold current density InGaAsN QW lasers were realized with improved temperature characteristics [13].

2. Optical and structural characterization on InGaAsN–InGaAsP

All the InGaAsN QW samples were grown on nominal exact (100) GaAs substrate by low-pressure metalorganic chemical vapor deposition (MOCVD). Trimethylgallium, trimethylindium and trimethylaluminum were used as the group III sources and AsH_3, PH_3, and U-Dimethylhydrazine were the group V precursors. The material composition was confirmed by high-resolution X-ray diffraction as well as room-temperature photoluminescence (PL) experiments. Material optical and structural properties were characterized by atomic force microscopy (AFM) and PL experiments. In both AFM and PL studies, structures with a highly compressive-strained ($\Delta a/a = 2.7\%$) 60 Å $Ga_{0.6}In_{0.4}As_{0.995}N_{0.005}$ QW under a growth temperature of 530°C were utilized. The growth rate of the InGaAsN QW was 1.28 μm/h. The N composition in the QW was calibrated by secondary ion-mass spectroscopy measurements.

2.1. PL experiments and results

The PL samples consisted of a 3000 Å GaAs confinement region, $Al_{0.74}Ga_{0.26}As$ top and bottom cladding layers and a tensile-strained transition layer of 30 Å $GaAs_{0.67}P_{0.33}$ grown at 700°C for improving the AlGaAs–GaAs interface quality [3]. This $GaAs_{0.67}P_{0.33}$ layer was found to be crucial for realizing high material quality of the highly strained InGaAsN QW grown on a high Al content (74%) bottom cladding layer. The barriers surrounding the InGaAsN QW were 70 Å lattice-matched $In_{0.3}Ga_{0.7}As_{0.4}P_{0.6}$ also grown at 530°C with bandgap energy of 1.62 eV. The growth rate and V/III ratio for the InGaAsP barrier was 1.38 μm/h and 288, respectively. The detailed structure for this study is shown in Fig. 1a. A control sample with identical QW composition and thickness for comparison purposes was also grown except the InGaAsP barriers were replaced with 100 Å GaAs layers followed by 75 Å $GaAs_{0.85}P_{0.15}$ strain compensation layers on each side of the QW, as shown in Fig. 1(b). Growth pausing annealing duration ranging from 3 to 21 s was applied at the interfaces between the QW and barriers under a low AsH_3 flow of 10 sccm in order to decide the optimum pause time (5200 sccm total hydrogen flow and AsH_3 partial pressure of 0.4 mbar). However, no growth pause annealing was utilized for the InGaAsN–GaAs–GaAsP control sample during MOCVD growth.

The measured room-temperature PL spectrum from the InGaAsN–InGaAsP structures with different pause time of 3–21 s is shown in Fig. 2 [9]. A dramatic increase of 25 times in PL intensity was observed when the pause time increases from 3 s to an optimized value of 14 s. Moreover, no significant wavelength shift was found, indicating a different mechanism of growth pause annealing from the post-growth thermal annealing process, in which a wavelength blue shift is commonly observed [5–7]. Slight emission wavelength fluctuations of 1.246–1.254 μm in this PL study are believed to be due to growth run-to-run variations.

Although a significant improvement of material quality was obtained by utilizing growth pause annealing as shown in Fig. 2, the optical quality of the InGaAsN–InGaAsP QW structure is still inferior

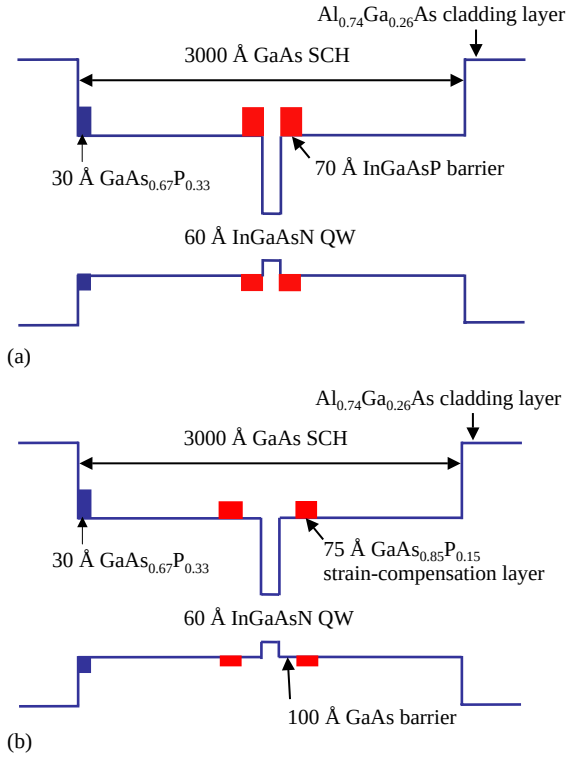

Fig. 1. Schematic band diagram of a single 60 Å $In_{0.4}Ga_{0.6}As_{0.995}N_{0.005}$ QW with (a) 1.62 eV $In_{0.3}Ga_{0.7}As_{0.4}P_{0.6}$ direct barriers and (b) GaAs direct barriers with $GaAs_{0.85}P_{0.15}$ strain compensation layers. Growth pause annealing treatment was applied at the interfaces between the QW and barriers.

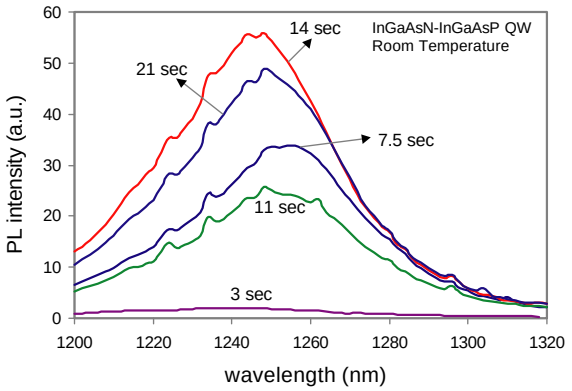

Fig. 2. PL spectra of the InGaAsN–InGaAsP structures with various growth pause time ranging from 3 to 21 s, which show a dramatic improvement of PL intensity while no significant change in emission wavelength was observed.

to that of the conventional InGaAsN–GaAs QW structure (control sample) with one order of magnitude lower PL intensity. The PL spectra of both structures are shown in Fig. 3 and the emission wavelengths are 1245 and 1274 nm, respectively, with the wavelength shift arising as a result of the quantum size effect. To be compatible with the InGaAsN growth conditions, we have grown the InGaAsP barriers at a temperature of 530°C, which likely is within the miscibility gap for this composition InGaAsP [14]. This resulted in a relatively poor material quality of the InGaAsP, possibly leading to higher nonradiative monomolecular recombination processes (i.e. lower PL intensity).

A similar improvement in PL intensity after growth pause annealing was also observed for structures consisting of InGaAsN QW and $GaAs_{0.85}P_{0.15}$ barriers [9]. The fact that the growth pause annealing only leads to improvement in structures with phosphorous-containing barriers (InGaAsP and GaAsP), not conventional GaAs barriers, indicates phosphine carry-over as a possible underlying effect. However, we found comparable PL intensity for InGaAs–InGaAsP QW structures with and without growth pause, indicating only structures containing N require the growth pause.

In order to identify the effect of the growth pause on either the InGaAsN-to-InGaAsP or InGaAsP-to-InGaAsN interface, two samples with a growth interruption of 14 s applied at either side

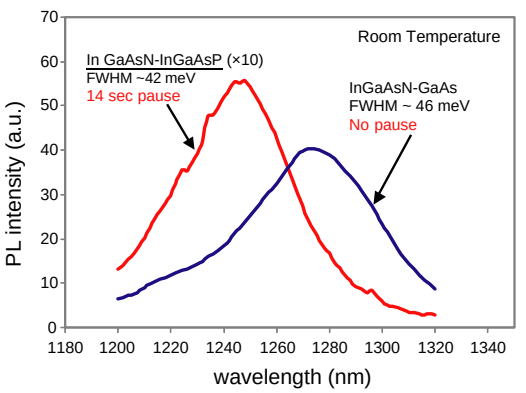

Fig. 3. PL spectrum comparison between the optimized InGaAsN–InGaAsP QW structure and the control sample of InGaAsN–GaAs.

of the QW were grown and also characterized with room-temperature PL experiments. It was found that the sample with a growth pause on the lower InGaAsP-to-InGaAsN interface had comparable PL intensity with the sample having pauses on both sides. On the contrary, extremely low PL intensity was observed when a growth pause was introduced only to the top interface, indicating the difficulty of growing highly strained InGaAsN QW may be related to a relatively rough InGaAsP surface, presumably due to the low growth temperature of 530°C.

2.2. AFM experiments and results

This strong relation between interface roughness and material optical quality can be further confirmed by the following AFM experiments. Two experiments were also conducted using a contact-mode AFM in order to clarify the mechanism of growth pause annealing. In the first AFM experiment, two structures were compared; sample A, consisting of a lower barrier of $In_{0.3}Ga_{0.7}As_{0.4}P_{0.6}$ and sample B, where the lower barrier was replaced with GaAs. Both samples were capped by 2 nm GaAs on the top of the InGaAsN QW as shown schematically in Figs. 4(a) and (b). A growth pause of 14 s, an optimal value determined from the PL study, was used in the growth of sample A. No growth pause was used for sample B. In the second AFM experiment, samples C–E all have identical structures with lower and upper InGaAsP barriers as shown in Figs. 4(c)–(e) and were cooled down under a flow of AsH_3 and PH_3. The growth pause annealing time was the only difference between these three samples and they were 3, 7.5 and 14 s for samples C, D and E, respectively. Although the post-growth cooling down process may alter the surface morphology, nevertheless, these samples allow a comparison study for understanding the effects of QW growth pause annealing duration on the surface morphology.

Figs. 4(a) and (b) show the AFM images of samples A and B with a size of $20\,\mu m \times 20\,\mu m$. Root-mean-square (RMS) surface roughness of these two samples were found to be 1.27 and 1.00 nm, respectively, suggesting a smoother surface of InGaAsN–GaAs compared to InGaAsN–InGaAsP even when an optimized growth pause was applied to sample A. This AFM data supports the PL result, in which the control sample exhibits roughly 10 times higher PL intensity as shown in Fig. 3. These data suggest that the surface morphology and optical luminescence properties of the InGaAsN QW are strongly related. The InGaAsN–GaAs structure exhibits both a smoother surface and higher PL intensity than the InGaAsN–InGaAsP structure. Similar behavior of interfacial undulation between an InGaAsN QW and GaAsN barriers were also reported by Li et al., for which a strong correlation between PL line width and interface undulation was presented [15].

The second AFM experiment was conducted on samples C, D and E and the resulting AFM images are showed in Figs. 4(c), (d) and (e), respectively. The RMS surface roughness reduced from 1.2 nm for the 3-s pause sample to 0.6 nm for the 14-s pause sample, showing a reduction of 50%. In Figs. 5(a) and (b), the influence of growth pause annealing time on RMS surface roughness, PL intensity and PL spectrum full-width half-maximum (FWHM) are summarized, showing the relationship between surface morphology and the optical quality of the InGaAsN QW on the growth pause annealing (i.e. increased PL intensity and reduced RMS roughness as pause time increases within the studied range).

In addition to a reduction in RMS roughness, other changes in surface morphology are noticeable and may also play a role in the improved material quality. As shown in Fig. 4(c), the 3-s pause sample exhibits a large number of surface pits with an average configuration 0.8 μm in diameter and 3 nm in depth. A similar observation was also published by Baskar et al. on a MOCVD-grown structure consisting of a 7 nm InGaAsN QW with GaAs pre-layer and cap layer [16], where they found that by carefully choosing growth conditions (growth temperature, DMHy flow), the density of surface pits could be greatly reduced. Here, we investigated the dependence of pit density on the growth pause annealing. Comparing Figs. 4(c)–(e), the number of surface pits decreases substantially as the pause time was extended to 14 s. The pit density of these three samples are 1.23×10^7, 7.5×10^6 and $2.75 \times 10^6\,cm^{-2}$, respec-

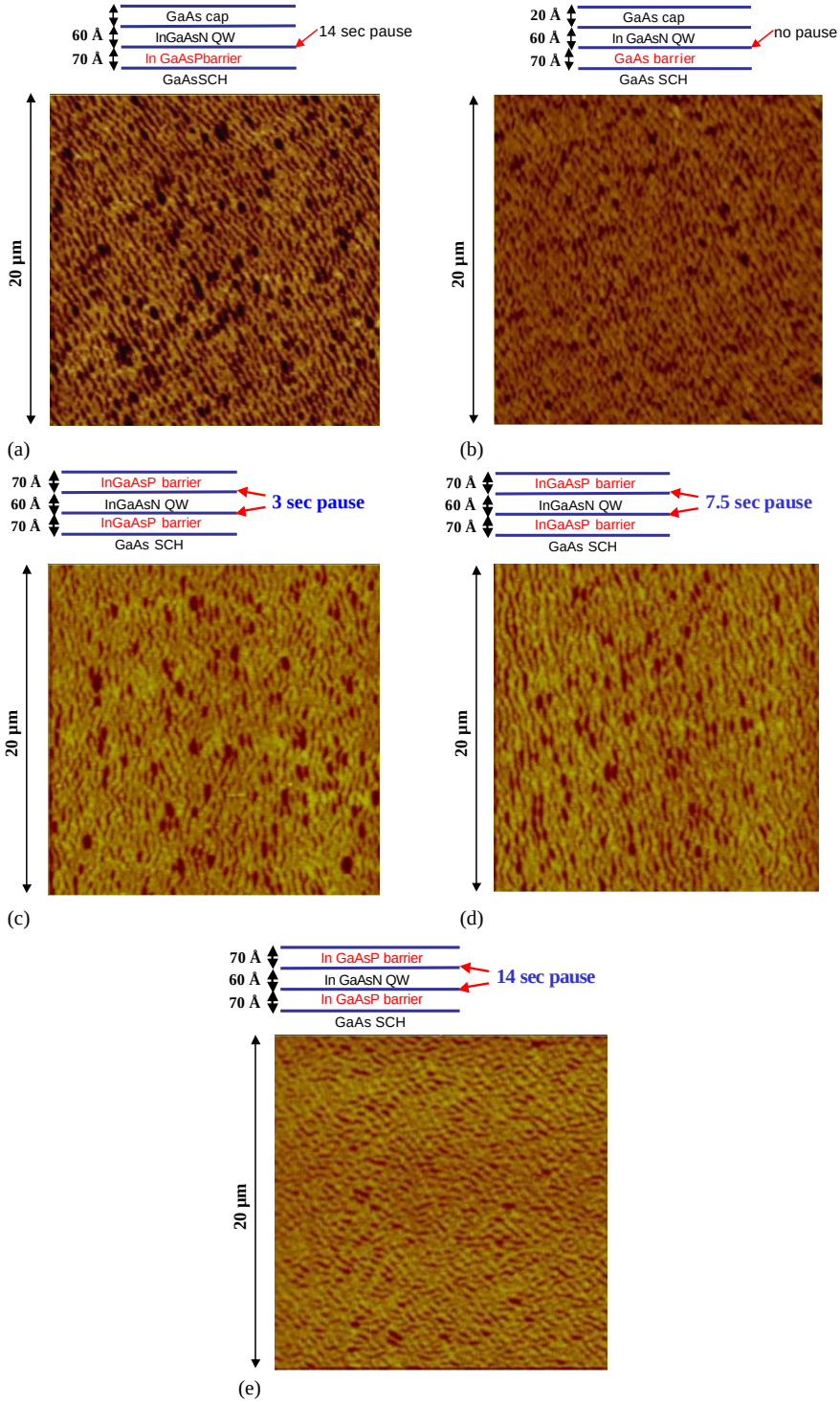

Fig. 4. The AFM images and the corresponding InGaAsN QW structures for studying the effects of different barriers of InGaAsP and GaAs (Figs. 4(a) and (b)) and different growth pause time of 3, 7.5 and 14 s (Fig. 4(c)–(e)) on surface morphology.

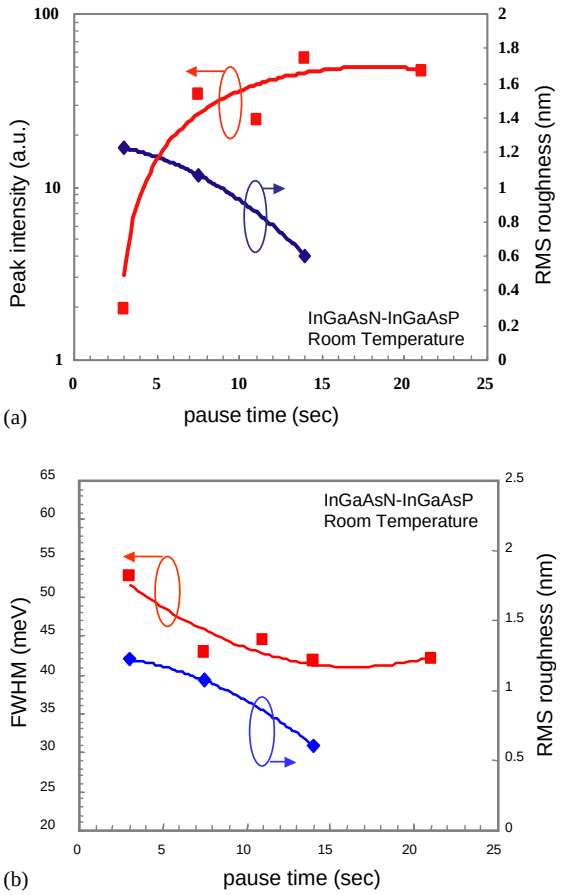

Fig. 5. RMS surface roughness, PL intensity and PL spectrum FWHM as functions of growth pause time, showing a consistent relation between surface morphology and optical qualities of InGaAsN QW on growth pause annealing effect.

tively. In addition, an ordered wire-like pattern was formed on the sample surface with the 14-s growth pause (Fig. 4(e)). By contrast, the other two samples with shorter pauses (Figs. 4(c) and (d)) revealed a more random surface features. Also shown in Fig. 4 (b), the InGaAsN–GaAs QW structure exhibits a similar surface atomic arrangement while no growth pause was introduced.

3. InGaAsN–InGaAsP QW lasers

InGaAsN QW lasers with InGaAsP (Fig. 1(a)) and GaAs (Fig. 1(b)) direct barrier were fabricated into broad area structure with a stripe width of 100 μm. Ti–Pt–Au and Ge–Ni–Au alloys were deposited and annealed to form the p- and n-type Ohmic contacts, respectively. The lasing characteristics were measured within a temperature range of 10–100°C under a 1% duty cycle (5 μs pulse width and 2 kHz repetition rate). These two structures provide different conduction and valence band offsets, suggesting an opportunity to investigate the relation between carrier confinement and temperature characteristics of the InGaAsN QW lasers. The valence band offsets (ΔE_v) are calculated approximately as 100 and 150 meV, respectively, with the assumption of ΔE_c:ΔE_v equal to 80:20 applied to both cases [11]. Since the electron confinement is very large for all three cases (>450 meV), electron leakage can therefore be neglected. Optimized growth pause annealing time duration was 14 s for the InGaAsN–InGaAsP interfaces while no growth interruption was introduced to the InGaAsN–GaAs interface. Typical temperature characteristics of threshold current density (J_{th}) of these structures (2 mm cavity length) are shown in Fig. 6. At room temperature, the threshold current densities and lasing wavelengths are 229, 441 A/cm^2 and 1.295, 1.26 μm for the InGaAsN–GaAs and InGaAsN–InGaAsP lasers, respectively [10]. Note that although InGaAsN–InGaAsP structure exhibited PL intensity 10 times lower than InGaAsN–GaAs structure, a reasonable J_{th} (only two times higher) was observed for this laser. Higher T_0 of 128 and 98 K for the InGaAsP barrier structure were obtained in the temperature range of 10–50°C and 50–100°C, comparing to the results of 97 and 75 K of the conventional GaAs-barrier QW laser structure. However, in this preliminary result, the improved T_0 values come at the expense of increased J_{th}, indicating further improvements are required in growth optimization of the high-bandgap InGaAsP ($E_g \sim 1.62$ eV).

4. Summary

In conclusion, PL and AFM experiments were conducted to examine the InGaAsN QW structure with large energy bandgap material InGaAsP

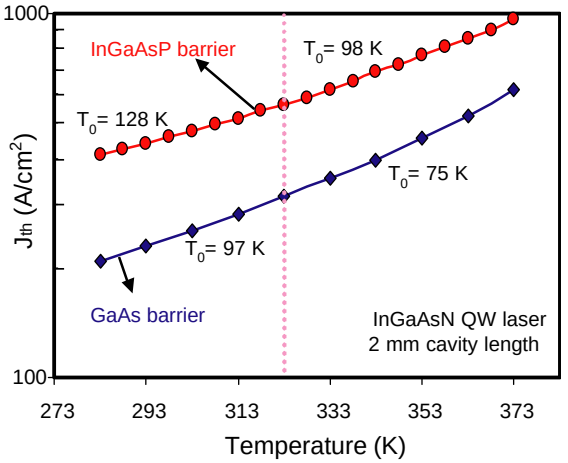

Fig. 6. Threshold current density as functions of heat sink temperature of InGaAsN QW lasers with InGaAsP barrier (structure in Fig. 1(a)), and GaAs barrier (structure in Fig. 1(b)).

($E_g = 1.62$ eV) as barrier layers. It was found that a growth pause annealing improved both material surface morphology and optical quality significantly. With an optimum growth pause of 14 s, the PL intensity increases as much as 25 times and the RMS surface roughness reduces by 50%, compared with the sample under a 3-s pause growth annealing treatment. Moreover, a reduced surface pit density and ordered wire-like pattern were also observed for the optimized growth conditions. Preliminary results on InGaAsN-active diode lasers employing InGaAsP barrier material indicate the performance limited by nonradiative recombination as a result of poor material quality of low-temperature-grown high-bandgap InGaAsP.

Acknowledgements

The authors gratefully acknowledge Dr. M. Tan, Dr. D.P. Bour, Dr. Y.L. Chang, and Dr. T. Takeuchi of Agilent Technologies Laboratories, Palo Alto, CA, for helpful support and discussions.

References

[1] M. Kondow, T. Kitatani, S. Nakatsuka, M.C. Larson, K. Nakahara, Y. Yazawa, M. Okai, K. Uomi, IEEE J. Select. Topic Quantum Electron. 3 (1997) 719.
[2] D.A. Livshits, A.Yu. Egorov, H. Riechert, Electron. Lett. 36 (2000) 1381.
[3] N. Tansu, N.J. Kirsch, L.J. Mawst, Appl. Phys. Lett. 81 (14) (2002) 2523.
[4] N. Tansu, L.J. Mawst, IEEE Photon. Technol. Lett. 14 (2002) 444.
[5] M. Kawaguchi, T. Miyamoto, S. Minobe, F. Koyama, K. Iga, Proceedings of the 14th International Conference of Indium Phosphide and Related Materials, Stockholm, Sweden, 12–16 May 2002, Paper P1-37.
[6] W. Li, J. Turpeinen, P. Melanen, P. Savolainen, P. Uusimaa, M. Pessa, Appl. Phys. Lett. 78 (1) (2001) 91.
[7] E. Tournie, M.A. Pinault, A. Guzman, Appl. Phys. Lett. 80 (22) (2002) 4148.
[8] V. Gambin, V. Lordi, W. Ha, M. Wistey, T. Takizawa, K. Uno, S. Friedrich, J. Harris, J. Crystal Growth 251 (2003) 408.
[9] N. Tansu, J.-Y. Yeh, L.J. Mawst, Appl. Phys. Lett. 82 (18) (2003) 3008.
[10] J.-Y. Yeh, N. Tansu, L.J. Mawst, Proceedings of the 15th International Conference of Indium Phosphide and Related Materials, Santa Barbara, CA, USA, 12–16 May 2003, Paper WA2.3.
[11] M. Hetterich, M.D. Dawson, A.Yu. Egorov, D. Bernklau, H. Riechert, Appl. Phys. Lett. 76 (8) (2000) 1030.
[12] N. Tansu, L.J. Mawst, Appl. Phys. Lett. 82 (10) (2003) 1500.
[13] N. Tansu, J.Y. Yeh, L.J. Mawst, Appl. Phys. Lett. 83 (11) (2003) 2112.
[14] B. deCremoux, P. Hirtz, J. Ricciardi, Inst. Phys. Conf. Ser. 56 (1981) 115;
G.B. Stringfellow, Organometallic Vapor-Phase Epitaxy, 2nd Edition, Academic Press, San Diego, 1999.
[15] L.H. Li, G. Patriarche, A. Lemaitre, L. Largeau, L. Travers, J.C. Harmand, J. Crystal Growth 251 (2003) 403.
[16] K. Baskar, P. Sundgren, O. Douheret, G. Landgren, J. Crystal Growth 248 (2003) 431.